Anomalous Magnetism of Uranium(IV)-Oxo and -Imido Complexes Reveals Unusual Doubly- Degenerate Electronic Ground States

DOI:
10.1016/j.chempr.2021.05.001

Document Version
Accepted author manuscript

Anomalous Magnetism of Uranium(IV)-Oxo and -Imido Complexes Reveals Unusual Doubly-Degenerate Electronic Ground States

John A. Seed,[1] Letitia Birnoschi,[1] Erli Lu,[1] Floriana Tuna,[1,2] Ashley J. Wooles,[1] Nicholas F. Chilton,[1,*] and Stephen T. Liddle[1,3]*

[1] Department of Chemistry, The University of Manchester, Oxford Road, Manchester, M13 9PL, UK.

[2] Photon Science Institute, The University of Manchester, Oxford Road, Manchester, M13 9PL, UK.

[3] Lead Contact

*Correspondence Email: steve.liddle@manchester.ac.uk; nicholas.chilton@manchester.ac.uk

SUMMARY

A fundamental part of characterising any metal complex is understanding its electronic ground state, for which magnetometry provides key insight. Most uranium(IV) complexes exhibit low-temperature magnetic moments tending to zero, consistent with a non-degenerate spin-orbit ground state. However, there is a growing number of uranium(IV) complexes with low-temperature magnetic moments ≥1 μ_B, suggesting a degenerate ground state, but the electronic structure implications and origins have been unclear. We report uranium(IV)-oxo and -imido complexes with low-temperature magnetic moments ca. 1.5-1.6 μ_B and show that they exhibit near-doubly degenerate spin-orbit ground states. We determine that this results from the strong point-charge-like donor properties of oxo and imido anions generating pseudo-symmetric electronic structures, and that traditional crystal field arguments are useful for understanding electronic structure and magnetic properties of uranium(IV). This suggests that a significant number of uranium(IV) complexes might benefit from a close re-evaluation of the nature of their spin-orbit ground states.

INTRODUCTION

The nature of coordinated ligands and the formal oxidation state of uranium modulate the key effects of inter-electronic repulsion (IER), spin-orbit coupling (SOC), and the crystal field (CF), which together determine the electronic structure of any uranium complex.[1] Some or all of these effects can be of comparable magnitudes where early actinides are concerned. Therefore, more than anywhere else in the periodic table, the electronic structure of early actinides can be intrinsically very complex and challenging to study, yet it is fundamentally important to understand because it dictates the nature of the electronic ground state, which in turn is intimately connected to the bonding, reactivity, and physicochemical properties of a molecule. As uranium is a central element in civil nuclear energy production,[2-4] resolving the long-standing challenge of nuclear waste could in the future utilise selective extraction methods that exploit a better understanding of covalency differences in uranium-ligand bonding, which are intrinsically connected to the underlying electronic structure.

One of the most valuable and informative methods for characterising paramagnetic open-shell uranium complexes is by variable-temperature magnetometry, since this can give direct insight into the nature of the ground state and formal oxidation state. The free uranium(IV) ion, which has a ground $^3H_4$ ground state in Russell-Saunders formalism, is predicted to exhibit a magnetic moment of 3.58 μ_B, however due to significant CF effects in molecular complexes this is often around 2.0 – 2.5 μ_B at 298 K and usually decreases smoothly towards ~0.3-0.5 μ_B at 2 K;[5-8] the decrease is due to depopulation of excited CF states into a magnetic singlet ground state (A) with appreciable temperature independent paramagnetism (TIP);[7,9] note that this is not an $S = 0$ spin-singlet ground state, but rather a singly-degenerate spin-orbit state – though rare examples of complexes with $S = 0$ ground states do exist, *e.g.* $[(C_5Me_4H)_3UNO]$.[9,10] Such behaviour is known for O_h-symmetric $[UX_6]^{2-}$,[5,11,12] and occurs because the $J = 4$ spin-orbit multiplet splits into A_1, E, T_1, and T_2 irreducible representations in O_h symmetry,[13] for which the A_1 singlet state is lowest in energy.[11,14]

The A_1 state is diamagnetic because it is composed of approximately 58% $m_J = 0$, 21% $m_J = -4$, and 21% $m_J = +4$,[11] where the $m_J = 0$ state is itself diamagnetic and the equal contributions of the $m_J = \pm 4$ states cancel each other out; this can also be mapped to spin and orbital contributions to the m_J states, which can be calculated *via* Clebsch-Gordan coefficients[15] and measured experimentally.[12] On the other hand, compounds of different symmetry may not show a decrease to near-zero magnetic moment at low temperature, signifying the presence of a degenerate paramagnetic ground state (E). For example, uranocene, $[U(\eta^8\text{-}C_8H_8)_2]$,[16] has a magnetic moment of ~2.6 μ_B at 300 K[17] that decreases to 1.35 μ_B at 4 K:[18] in this case, the D_{8h} symmetry of the solid-state structure splits the $J = 4$ spin-orbit multiplet into A_1, E_1, E_2, E_3, and $B_1 + B_2$ irreducible representations, for which E_3 ($m_J = \pm 3$) is the ground state.[19-21]

Outside of "simple" high-symmetry complexes, sufficiently low-symmetry coordination geometries will usually exhibit a singlet (A) spin-orbit ground state;[5,7,22] this is because uranium(IV) has two unpaired electrons and is thus a non-Kramers ion, and hence there is no requirement for any electronic degeneracies in the $J = 4$ spin-orbit multiplet after the action of the CF, because the CF effect for 5f-orbitals is significant. However, there are now a growing number of formally low-symmetry uranium(IV) complexes where with innocent ligands the low-temperature (<2 K) magnetic moments are quite high (≥1 μ_B),[23-39] suggesting that something is differentiating these complexes. Empirically, singlet ground states tend to be observed with monoanionic ligands, regardless of the (pseudo-)symmetry, and higher magnetic moments have increasingly been observed at low-temperature when stronger di- or tri-anionic ligands are present, implying a (pseudo-)doublet (E) spin-orbit ground state.[22] Hence, there is increasing evidence that there is a threshold CF strength for which high-symmetry arguments, and thus a switching of spin-orbit ground state, might be invoked.

Previously, we reported that the *N*-heterocyclic olefin $H_2C{=}C(NMeCH)_2$ reacts with $[U^{III}(N'')_3]$ (N″

= $N(SiMe_3)_2$) to produce the mesoionic carbene complex $[U(N'')_3\{CN(Me)C(Me)N(Me)CH\}]$ that exhibits a $U^{III}\rightarrow C$ 1-electron back-bond interaction.[40] Seeking to widen the family of uranium mesoionic carbene complexes we targeted uranium(V) derivatives. However, we find instead that the basic reactivity properties of the *N*-heterocyclic olefin become a complicating factor, promoting cyclometallation and disproportionation reactions, generating rare examples of uranium(IV)-oxo and -imido complexes. We find that these complexes exhibit unusually high low-temperature magnetic moments, for complexes formally of C_1 symmetry, and so we investigated the electronic structure of these complexes to address the nature of the electronic ground state. This has permitted us to unambiguously verify that pseudo-C_3-symmetric uranium complexes with a strong axial ligand can have paramagnetic pseudo-doublet (E) spin-orbit ground states, showing that traditional CF symmetry arguments can dictate the electronic structure and magnetic properties when strong enough point-charge-like ligands are coordinated to uranium.

RESULTS AND DISCUSSION

Synthetic considerations and spectroscopic characterisation. Treatment of pre-prepared $[U^{V}(O)(N'')_3]$ (N″ = $N(SiMe_3)_2$, **1**)[26] or *in situ* prepared $[U^{V}(NSiMe_3)(N'')_3]$ (**2**, by oxidation of $[U^{III}(N'')_3]$ with N_3SiMe_3) with half an equivalent of the *N*-heterocyclic olefin $H_2C{=}C(NMeCH)_2$ (**3**) in either diethyl ether or hexane, produces, after work-up and recrystallisation, brown needles of the uranium(IV)-oxo and -imido complexes $[U^{IV}(O)(N'')_3][(Me)C(NMeCH)_2]$ (**4**) or $[U^{IV}(NSiMe_3)(N'')_3][(Me)C(NMeCH)_2]$ (**5**), respectively, Scheme 1. The crystalline yields of **4** and **5** are both 13%, which is low because **4** and **5** decompose in solution affording $HN(SiMe_3)_2$ and unidentified and intractable by-products and because their formation results from disproportionation reactions where the uranium(VI)-cyclometallate complexes $[U^{VI}(O)(N'')_2\{N(SiMe_3)(SiMe_2CH_2)\}]$ (**6**)[41] for **4** and $[U^{VI}(NSiMe_3)(N'')_2\{N(SiMe_3)(SiMe_2CH_2)\}]$ (**7**) for **5**, respectively, form concomitantly, thus limiting the maximum yield in each case to 50%.

When **1** or **2** are treated with one equivalent of **3**, the uranium(V)-cyclometallate complexes $[U^{V}(O)(N'')_2\{N(SiMe_3)(SiMe_2CH_2)\}][(Me)C(NMeCH)_2]$ (**8**) and $[U^{V}(NSiMe_3)(N'')_2\{N(SiMe_3)(SiMe_2CH_2)\}][(Me)C(NMeCH)_2]$ (**9**), respectively, are formed quantitatively (see Supplemental Information). Complexes **8** and **9** decompose when they are left in solution for prolonged periods, with complete decomposition found after 60 and 15 minutes, respectively. However, if **8** or **9** are treated quickly with one equivalent of **1** or **2**, respectively, then 1:1 mixtures of disproportionated **4**:**6** or **5**:**7** are formed analogously to the half equivalent reactions with **3** above.

The reactions between **1** or **2** with half an equivalent of **3** clearly produce 1:1 mixtures of **4**:**6** or **5**:**7**, respectively, as a result of disproportionation and cyclometallation. The reactions of **1** and **2** with one equivalent of **3** provide insight into the likely mechanism of this reaction, since cyclometallated **8** or **9** are formed in this situation, but only after addition of further **1** or **2**, which then essentially renders the **1**/**2**:**3** ratio 1:0.5, does disproportionation occur. The cyclometallation can be accounted for by basic **3** promoting C-H activation and H-abstraction, and that the extra cyclometallate donor destabilises the uranium(V) ions in **8** and **9**, as evidenced by their otherwise rapid decomposition, such that oxidation to uranium(VI) is more favourable for the cyclometallate formulation at the expense of an anionic formulation by reduction for the uranium-oxo and -imido components of **4** and **5**. Certainly, the absence of D-incorporation for reactions conducted in D_6-benzene are consistent with this, and $[U^{V}(O)(N'')_2\{N(SiMe_3)(SiMe_2CH_2)\}][MePPh_3]$,[41] that is essentially **8** but with a different counter-cation, is known to be easily oxidised ($E_{1/2}$ = –0.85 V vs. $[Cp_2Fe]^{0/+}$).

Once isolated, **4** and **5** are poorly soluble in aromatic solvents, and they decompose in ethers, but NMR spectroscopic data (Figures S1 to S4) are consistent with their uranium(IV) formulations and show no evidence of D-incorporation from deuterated solvent (benzene). The six trimethylsilyl groups resonate as one singlet per complex in the ^{1}H NMR spectrum, indicating a symmetric

species on the NMR timescale. However, these are shifted upfield relative to **1** and **2** in agreement with the increased electron density at the uranium(IV) centres. For **5**, the trimethylsilylgroup of the axial imido ligand is observed in the ^{1}H NMR spectrum at –12.55 ppm, but no ^{1}H NMR resonance for the [M=NSi*Me*$_3$] group for **2** has been reported so no comparison can be made; however, the ^{29}Si NMR spectra of **4** and **5** exhibit weak resonances at –37.74 and –90.74/–131.19 ppm, respectively, which is within the range of reported ^{29}Si chemical shifts for uranium(IV) complexes.[42] Complexes **6** and **8** were identified by comparison of NMR spectra (Figures S5 to S7) of reaction mixtures compared to published data and $[U^{V}(O)(N'')_2\{N(SiMe_3)(SiMe_2CH_2)\}][MePPh_3]$,[41] respectively. Complex **9** was identified by NMR spectroscopy with reference to **8**, but **7** could not be unambiguously spectroscopically identified, most likely because the imido does not stabilise the uranium(VI) oxidation state as well as an oxo, but its fleeting existence seems all but assured given the parallels between these oxo and imido systems with five of the six reaction partners identified.

The IR (Figures S8 and S9) and UV/Vis/NIR spectra (Figures S12 to S15) of **4** and **5** were recorded. Unfortunately, the oxo and imido linkages of **4** and **5** would be anticipated to fall in the region 800-1,000 cm^{-1}, which has been shown to often contain absorptions from the silyl-amide complicating analysis.[26] The UV/Vis/NIR spectra of **4** and **5** are dominated by strong charge transfer bands from the UV region to around 20,000 cm^{-1}. Across the range 20,000-5,000 cm^{-1} the spectra are dominated by multiple but weak (ε <80 M^{-1} cm^{-1}) absorptions that are characteristic of Laporte forbidden f-f transitions of uranium(IV) ions, in accordance with the pale brown colour of both complexes.[1,6,43]

Solid state structural characterisation. In order to confirm the formulations of **4** and **5**, their solid-state structures were determined, Figure 1. In gross terms each are very similar, with a separated ion pair formulation and four-coordinate uranium ions. The geometry about uranium in **4** is essentially

trigonal monopyramidal, with an average O-U-N_{amide} angle of 96.8(3)° and an average N_{amide}-U-N_{amide} angle of 118.6(3)°, such that the uranium ion lies only 0.279(4) Å above the plane defined by the three N_{amide} centres. In contrast, **5** exhibits a pseudotetrahedral geometry about uranium, with an average N_{imido}-U-N_{amide} angle of 102.39(2)° and an average N_{amide}-U-N_{amide} angle of 115.53(2)°. Thus, the geometries of tetravalent **4** and **5** largely mirror those of pentavalent **1** and **2**, respectively. The U-N_{amide} distances in tetravalent **4** and **5** span the ranges 2.346(7)-2.351(7) and 2.359(4)-2.368(4) Å, respectively. For comparison, the U-N_{amide} distances in pentavalent **1** [2.235(1)-2.244(2) Å][26] and **2** [av. 2.295(10) Å][44] are significantly shorter. For **4**, the U-O distance is significantly longer than that of **1** [1.882(6) vs. 1.817(1) Å, respectively] and the U-N_{imido} distance in **5** is significantly longer than that of **2** [1.985(4) vs. 1.910(16) Å, respectively]. More widely, the U-O distance in **4** is comparable to that of [U{OK(18-crown-6)}$(N'')_3$] [1.890(5) Å][45] and the U-N_{imido} bond length in **5** is comparable to those of [U(NDipp)Cl_2(^{t}Bu$_2$bpy)$(THF)_2$][46] and [K][U(=NCPh$_3$){N(SiMe$_3$)$_2$}$_3$][47] [1.981(2) Å and 1.9926(14) Å, respectively]. These structural features all support the uranium(IV) formulations of **4** and **5**.

Magnetometric characterisation. Powdered samples of **4** and **5** immobilised in eicosane were studied by variable-temperature SQUID magnetometry, Figures 2, S10 and S11. Complexes **4** and **5** exhibit magnetic moments of 2.88 and 3.01 μ_B at 300 K, respectively. These values are both lower than the theoretical magnetic moment of 3.58 μ_B for one uranium(IV) ion, which is not uncommon, but they are clearly higher than the maximal magnetic moment of 2.54 μ_B for one uranium(V) ion, and are substantially higher than the reported magnetic moments of **1** and **2** (1.59 μ_B and 2.04 μ_B, respectively, at 300K). The magnetic moments of **4** and **5** decrease slowly, reaching 2.36 and 2.30 μ_B, respectively, at 20 K, and then decrease more rapidly reaching 1.54 and 1.46 μ_B, respectively, at 2 K, Figure 2. The data for **4** and **5** do not fit the 'classical' behaviour of uranium(IV),[1,6,48] that is the smooth continuous decrease in magnetic moment as the temperature is decreased and tending to

zero at low temperature, which prompted us to probe their electronic structures in detail in order to explain this observation.

Electronic structure calculations. The uranium(IV) ion has a ground $5f^2$ configuration, with $S = 0$ (singlet) and $S = 1$ (triplet) electron spin quantum numbers. In the absence of SOC, the Russell-Saunders terms arising from IER for this configuration are (in order of increasing energy) ^3H, ^3F and ^3P for $S = 1$ and ^1G, ^1D, ^1I and ^1S for $S = 0$. SOC mixes these terms, rendering L and S no longer good quantum numbers, and in the weak SOC limit the Russell-Saunders coupling scheme describes the total angular momentum with quantum number J; for the f^2 configuration, Hund's rules predict a 9-fold degenerate $^3H_4$ ground state with a first excited $^3F_2$ state at *ca.* 5,000 cm^{-1};[7] hence, the SOC is large enough that the first excited multiplet is not $^3H_5$ as it is for $4f^2$ Pr^{III}. Nonetheless, the ground $^3H_4$ multiplet is well separated from excited states such that consideration of this multiplet alone is likely to be sufficient to explain ground state properties such as magnetism. This free-ion picture is not an accurate depiction of the electronic structure in a coordination complex, as bonding to ligands hybridises the valence orbitals and removes much of the electronic degeneracy (*i.e.* CF splitting). In general for complexes of uranium, the energy scales of IER, SOC and CF can be similar, especially in the case of multiple bonding, and multi-reference *ab initio* electronic structure calculations have emerged as a reliable way to determine the electronic structure of such molecules.[9,49-51] With the present complexes in mind, we first outline the electronic structure of a hypothetical linear $[U^{IV}O]^{2+}$ cation, followed by a hypothetical C_{3v}-symmetric trigonal pyramidal $[U^{IV}OF_3]^-$ anion (F^- is chosen to mimic the monoanionic point charge of the N″ equatorial donors in **4** and **5**), and finally onto the full complexes **4** and **5**.

Here we take the opportunity to address a point of considerable confusion in the modern literature of the magnetism and electronic structure of 5f-element complexes. Great care must be taken when describing electronic states for these materials where IER, SOC and CF can all compete, especially

when it comes to the distinction between the molecular orbital and spin-orbit pictures. For instance, if the CF is weak compared to IER and SOC (much like the case for lanthanides) it is somewhat irrelevant to discuss orbital splitting and the only relevant currency is the spin-orbit states. On the other hand, if the CF is strong, then there is a possibility that electronic ground state will no-longer be the free-ion Hund's Rule high-spin state and instead be in a low-spin configuration (much like the situation common for d-block metals), and thus discussing the orbital splitting and electronic populations are crucial. Confusingly, the electronic states arising from both the spin-orbit picture and the "electrons-in-orbitals" picture are both associated with irreducible representations of the molecular point group, and thus a doubly-degenerate spin-orbit state could be described as "E" and so could a doubly-degenerate molecular orbital. Hence, one must always be clear what states are being discussed.

It is also important to note here that orbital energies are inherently a single-electron construct, and are not defined in a correlated multi-electron wavefunction. However, we can extract the effective orbital energies from the observed CF splitting of the ground $^3H_4$ spin-orbit multiplet, by recalling the origin of the Stevens operator equivalent method, which relates the multi-electron CF Hamiltonian to the single-electron CF Hamiltonian.[52] The CF Hamiltonian:

$$\hat{H}_{CF} = \sum_{k\,=\,2,4,6} \sum_{q\,=\,-k}^{k} B_k^q \theta_k \hat{O}_k^q$$

acts on the ground J = 4 multiplet, where B_k^q are the CF parameters (CFPs), θ_k are the operator equivalent factors and $\hat{O}_k^q$ are the Stevens operators (functions of the total angular momentum operators, $\hat{J}$); for the $^3H_4$ multiplet of the f^2 configuration, θ_2 = -52/2475, θ_4 = -4/5445 and θ_6 = 272/4459455.[53] The CFPs can be directly extracted from our CASSCF-SO calculations,[54] and, using this Hamiltonian, the same CFPs can be applied to the single-electron l = 3 basis to extract the effective 5f-orbital splitting due to the CF; in this case θ_2 = -2/45, θ_4 = 2/495 and θ_6 = -4/3861,[53] where the $\hat{O}_k^q$ are now written in terms of the single-electron orbital angular momentum operators, $\hat{l}$.

For a linear $[U^{IV}O]^{2+}$ cation where the U=O bond length is taken from the crystal structure of **4** (1.884 Å), the axial CF induced by the oxo anion splits the 5f-orbitals into the $C_{\infty v}$ irreducible representations: E_3 (ϕ) < E_2 (δ) < E_1 (π) < A_1 (σ), Figure 3, where ϕ, δ and π are linear combinations of the m_l functions ±3, ±2 and ±1, respectively, and σ is m_l = 0. Here, the ϕ and δ orbitals are formally non-bonding, while the π and σ orbitals are formally antibonding with respect to the U-O bond, which is the origin of the orbital ordering.[51] However, when the CF is smaller than IER and SOC, such as for **4** and **5** (see below), the effect of the CF on top of the IER+SOC states is to remove the degeneracy of the *J* multiplets. In $C_{\infty v}$ symmetry, the ground $^3H_4$ multiplet is split into four pseudo-doublets and one singlet, and for $[U^{IV}O]^{2+}$: E_4 (m_J = ±4) < E_3 (m_J = ±3) < A_1 (m_J = 0) < E_1 (m_J = ±1) < E_2 (m_J = ±2), Figure 4. Note that because the configuration has an even number of unpaired electrons, it is a non-Kramers system and hence a low symmetry CF could fully remove the degeneracy of the m_J states; thus, we refer to these doublets as pseudo-doublets to distinguish them from Kramers doublets.

For the C_{3v}-symmetric trigonal pyramidal complex $[U^{IV}OF_3]^-$, where the U=O and U-F bond lengths are taken from the crystal structure of **4** (U=O: 1.884 Å, average U-N: 2.348 Å), we have performed CASSCF-SO calculations with a 2 in 7 active space (see Methods). In C_{3v} symmetry the $^3H_4$ multiplet splits as 2 × A_1 (m_J = ±3, 0), A_2 (m_J = ±3) and 3 × E (m_J = ±4, ±2, ±1),[13] Figure 3. Parameterising this splitting of J = 4 with the CF Hamiltonian, only B_k^q with q = 0, 3 or 6 are non-zero as the CF Hamiltonian must reflect the point symmetry of the molecule,[13] Table S1. In C_{3v} symmetry the f-orbitals split as 2 × A_1 (σ, ϕ), A_2 (ϕ) and 2 × E (π, π, δ, δ), where the ϕ pair is now split and mixed with σ, and in this case can be physically understood as arising from the bonding/antibonding interactions with the equatorial ligands. When the CF Hamiltonian is recast into the l = 3 orbital basis, we find that the orbitals order as A_1 < E < A_2 < E < A_1, Figure 3.

Moving to complexes **4** and **5**, CASSCF-SO calculations with a 2 in 7 active space (see Methods) find characteristically similar results to the C_{3v} $[U^{IV}OF_3]^-$ complex, Figures 3 and 4. We find that the ground $^3H_4$ multiplet is well-isolated and that there is a pattern of three pseudo-doublets and three singlets, where the ground pseudo-doublet is dominated by $m_J = \pm4$ and ±1, and the first excited singlet is dominated by $m_J = 0$ and ±3, Tables S2 and S3, and Figure S16. Here, the deviation from exactly degenerate pseudo-doublets is due to the low-symmetry component of the CF (*i.e.* deviations from C_{3v} symmetry), where the magnitude of the low-symmetry perturbation directly influences the energy gaps within each pseudo-doublet. Magnetic data computed for **4** and **5** on the basis of our CASSCF-SO results show good overall agreement with experiment, but our calculations do not approach the correct low-temperature limit, Figure 2; this is particularly acute for the *M vs. H* data of **4**, Figure 5. From our CASSCF-SO calculations, the pseudo-doublet ground states are split on the order of 31 and 9 cm^{-1} for **4** and **5**, respectively. In the limit of a truly-degenerate doublet (*i.e.* in perfect C_{3v} symmetry), we would expect a rapid increase of the magnetisation at low fields as the states split, followed by a slower increase at higher fields (*i.e.* saturation-like), and in the opposite low-symmetry limit of a well-isolated singlet state, the magnetisation would be near-zero. For both complexes, the CASSCF-SO-calculated magnetisation data are lower than the experimental data, indicating that the splitting in the pseudo-doublet ground state is overestimated by our calculations. We believe the worse agreement between experimental and CASSCF-calculated *M vs. H* data for **4** compared to **5** is due compound **4** having *ca.* 20% larger CF splitting than **5** (Table S2 cf. Table S3), meaning the state-average CASSCF wavefunction is less accurate for the lower-lying states than for **5**. There is no significant change in magnetic properties resulting from increasing the size of the active space (8 in 13 active space that includes frontier bonding and anti-bonding orbitals of the U=E unit, Figures S17 to S20), which is consistent with previous computational studies of uranium(IV) compounds.[9]

Because the low-temperature magnetisation experiment probes only the lowest states, these data provide an experimental measure of the splitting of the ground pseudo-doublet. The CF Hamiltonian described above provides a flexible model that allows us to modify the CF to reproduce the experimental data and thus indirectly measure the ground state pseudo-doublet splitting. To calculate the magnetic properties, we use the following Hamiltonian in the PHI program:[55]

$$\hat{H} = \sum_{k\,=\,2,4,6} \sum_{q\,=\,-k}^{k} B_k^q \theta_k \hat{O}_k^q + \mu_B \vec{\hat{J}} \cdot \bar{\bar{g}} \cdot \vec{B}$$

where the second term is the Zeeman Hamiltonian, representing the interaction of the complex with the magnetic field, μ_B is the Bohr magneton, $\vec{B}$ is the magnetic field and $\bar{\bar{g}}$ is the effective *g*-matrix of the $J = 4$ ground multiplet. We note that this model implies a pure 5f angular momentum basis, and thus anisotropy and hybridisation effects can be approximated with $\bar{\bar{g}}$, whose principal values (g_x, g_y, g_z) are also obtained from CASSCF-SO:[56] these values are (0.71, 0.72, 0.76) and (0.73, 0.73, 0.77) for **4** and **5**, respectively, which is slightly reduced from the free-ion Landé factor for the $^3H_4$ ground multiplet $g_J = 4/5$.

Starting from the CASSCF-SO-calculated CFPs, Tables S4 and S5, we fit susceptibility and magnetisation data simultaneously by varying only a single CFP. From the resulting sets of parameters, we analyse those that reduce the initial residual error (as defined in PHI)[55] by at least 90%. Additionally, we assume that the initial CASSCF-SO-calculated electronic structure is a good initial guess, and so we discard optimised CFP sets that lead to drastic changes of the overall structure of the $J = 4$ multiplet. This is achieved by examining the root mean squared deviations (RMSD) of the CF energy levels and of the pseudo-doublet energy gaps, Table S6. The energies of the first two excited states of both complexes are shown in Table S7, and μ_{eff} *vs. T* and *M vs. H* curves derived for each possible set of modified CFPs are illustrated in Figures S21 and S22. All acceptable CFP sets give consistent results for the *M vs. H* data of **5** (Figure S22b and Table S7),

indicating a ground pseudo-doublet gap of approximately 8.5(1) cm^{-1} with the first excited singlet state at *ca.* 120(30) cm^{-1}. Despite having a large energy RMSD, the optimised B_6^3 results show the best agreement with the experimental μ_{eff} *vs. T* curve, Figure S22a, suggesting the second excited state lies slightly higher at *ca.* 198 cm^{-1}, while the ground pseudo-doublet states are separated by 7.9 cm^{-1}. For **4**, only 2 sets of optimised CFPs match our selection criteria, and both predict a ground pseudo-doublet gap of just under 7 cm^{-1} with the singlet state at *ca.* 190 cm^{-1}. We note that none of these models are "correct" parameterisations of the CF, but rather a means-to-an-end of approximating the experimental pseudo-doublet splitting.

Following our identification that **4** and **5** have near-degenerate E spin-orbit ground states, there are two pertinent questions: *i*) why do these complexes display high-symmetry-like electronic structures despite their formal low symmetry; and *ii*) why do these complexes have E ground states as opposed to A_1 or A_2 ground states (all permissible in C_{3v})?

The answer to *i*) appears to be predominantly related to the presence of di- or tri-anionic ligands;[23-39] indeed, we have previously found that pseudo-C_{3v} uranium(V) complexes with terminal nitrido- and oxo- ligands tend to behave as belonging to a high-symmetry point group, unlike what their C_1 structures would dictate.[51,57] We found that some of the nitrido- complexes have EPR-silent m_J = ±3/2 ground states (silent in true C_{3v} symmetry), with excited m_J = ±5/2 states observable by EPR (active even in true C_{3v} symmetry) lying within a few tens of cm^{-1};[51] given the very sensitive nature of EPR, and that we could only observe EPR transitions in the excited state, the ground m_J = ±3/2 states must be very pure. This corroborates the observation that the corresponding terminal oxo-complex has a m_J = ±3/2 ground state and is completely EPR silent.[57] Presumably this occurs because there is a hierarchy of influences on the overall CF potential: single strong donor atom >> trigonal equatorial donors > low symmetry perturbations; while for complexes lacking a single

strong donor atom, the competition between the "high" and "low" symmetry parts of the CF is enough to remove the appearance of high symmetry.

The answer to *ii)* depends on the nature of the coordination complex, but can be explained using a simple electrostatic model that has arisen to design high-performance single-molecule magnets.[58-60] Each of the spin-orbit m_J states of the free-ion $^3H_4$ term has an aspherical 5f electron distribution that can be calculated analytically.[61] For $m_J = 0$ and ±1 the shapes are distinctly prolate spheroidal, while for $m_J = \pm4$ the shape is distinctly oblate spheroidal; $m_J = \pm2$ and ±3 are neither oblate nor prolate. In the presence of a highly-charged and multiply-bonded anion like the oxo- or imido-groups in **4** and **5**, simple electrostatic arguments dictate that the $m_J = \pm4$ state should be lower in energy than the other m_J states, while $m_J = 0$ and ±1 would be higher in energy. Of course, however, the spin-orbit states must conform to the (pseudo-)symmetry of the complex and are thus linear combinations of the m_J states. As a reminder, in C_{3v} symmetry the states mix as 2 × A_1 ($m_J = \pm3$, 0), A_2 ($m_J = \pm3$) and 3 × E ($m_J = \pm4$, ±2, ±1),[13] Figure 4. Thus, if the presence of a strong point-charge-like donor atom would favour a $m_J = \pm4$ ground state, then this would be one of the E states. Conversely, if the complex had only equatorial coordination, then a $m_J = 0$ ground state would be favoured, leading to an A_1 ground state. To demonstrate this, we have performed CASSCF-SO calculations on the model $[U^{IV}OF_3]^-$ complex where we start from a situation where the F^- ligands are 47 Å away (*i.e.* the CF splitting is that of $[U^{IV}O]^{2+}$ with $C_{\infty v}$ symmetry, Figure 6 left) and move them in until they arrive at their positions in $[U^{IV}OF_3]^-$ studied above (U-F: 2.348 Å, C_{3v} symmetry, Figure 6 centre), and then move the O^{2-} ligand out from its initial position (U=O: 1.884 Å) to 38 Å away (*i.e.* the CF splitting is that of $[U^{IV}F_3]^+$ with D_{3h} symmetry, Figure 6 right); as expected we observe a flip from an E ground state to an A_1 ground state between $[U^{IV}OF_3]^-$ and $[U^{IV}F_3]^+$.

To test both *i)* and *ii)*, we have performed a CASSCF-SO calculation on **4** where we have removed the oxo- anion, *i.e.* $[U^{IV}(N'')_3]^+$, while maintaining the formal C_1 symmetry of the crystalline

geometry. We find that the ground state is well-described as $m_J = 0$ (*i.e.* A_1' of D_{3h}, Figure 6, right), and that the excited states are linear combinations of $m_J = \pm1$, ±2, ±3 and ±4, respectively, split by *ca.* 110, 20, 120 and 20 cm^{-1}, respectively (Table S8). The large splitting of 120 cm^{-1} between the $m_J = \pm3$ pair is expected in D_{3h} symmetry (Figure 6, right) due to the allowed B_6^6 crystal field parameter,[13] while the large splitting between the $m_J = \pm1$ states arises from low-symmetry perturbations (*i.e.* from non-zero $B_k^{\pm1,\pm2}$ terms due to structural elements with no, or at most two-fold, rotational symmetry). The presence of this large splitting should be compared to the splittings found between the E states in **4** which are (from CASSCF-SO) 30, 20 and 30 cm^{-1}, respectively, clearly showing that low-symmetry perturbations are less influential in the presence of a strong point-like donor atom.

In summary, we have demonstrated that treatment of oxo- and imido-triamide complexes of uranium(V) with an *N*-heterocyclic olefin results not in mesoionic carbene complexes but cyclometallation/disproportionation reactions that generate uranium(IV)-oxo and -imido anion complexes along with uranium(VI)-cyclometallates. The uranium(IV)-oxo and -imido complexes exhibit unusually high low-temperature magnetic moments for such low symmetry systems, that should exhibit magnetic singlet ground states, which prompted an in-depth analysis of their electronic structures using CASSCF-SO and CF methods benchmarked to low-temperature magnetisation and magnetic susceptibility experiments. The experimental magnetisation data indicate a pseudo-doublet (E) ground state for both compounds, split by *ca.* 7 and 8.5 cm^{-1} for **4** and **5**, respectively, determined by CF modelling of low temperature magnetometry data. These small splittings thus yield uncharacteristically large ground-state magnetic moments for formally C_1-symmetric species, owing to the presence of strong, formally 2^- point-charge-like oxo- and imido-ligands, along with relatively high pseudo-symmetry approaching C_{3v}. These data permit us to rationalise and confirm the basic principle that a singlet (A) spin-orbit ground state is usually the default for low-symmetry uranium(IV), but this can be flipped to a pseudo-doublet (E) spin-orbit

ground state when there are sufficiently strong ligands to dominate the CF. Lastly, this work suggests that there are likely many uranium(IV) complexes with E rather than A spin-orbit ground states on the basis that they exhibit low-temperature magnetic moments of $\geq 1\ \mu_B$ in the presence of strong axial-type donor ligands.

EXPERIMENTAL PROCEDURES

Resource Availability

Lead Contact

Further information and requests for resources and reagents, which may be subject to UK national export licence restrictions, should be directed to the Lead Contact, Stephen T. Liddle (steve.liddle@manchester.ac.uk).

Materials Availability

Compounds **4**-**9** can be produced following the procedures outlined below and in the Supplemental Information from standard reagents and procedures.

Data and Code Availability

Crystal data for **4** and **5** are available from the Cambridge Crystallographic Data Centre under CCDC: 1903812 and 1903813. Computational output is available on request.

Synthesis

All manipulations were carried out under an inert atmosphere of dry nitrogen using Schlenk or glove box techniques. Compounds were characterised by single crystal X-ray diffraction, NMR, IR, and UV/Vis/NIR spectroscopies, variable temperature SQUID magnetometry, elemental analysis, and CASSCF-SO methods. See the Supplemental Information for further details.

Preparation of [U^{IV}(O)(N")$_3$][(Me)C(NMeCH)$_2$] (4)

A solution of H_2C=C(NMeCH)$_2$ (0.05 g, 0.55 mmol) in Et_2O (5 ml) was added dropwise to a pre-cooled (–78 °C) red solution of [U^V(O)(N″)$_3$] (0.74 g, 1.00 mmol) in Et_2O (5 ml). The mixture was allowed to warm to room temperature slowly over 10 minutes, resulting in a colour change to brown. The reaction mixture was stirred for 1 min at room temperature. After which, the volume of the solution was reduced *in vacuo* by half, filtered using a double-wrapped cannula, and subsequently layered with hexane (5 ml). Storage of the solution at –30 °C for 24 hours afforded **4** as brown needle crystals. Yield: 0.11 g, 13%. Anal. Calcd for $C_{24}H_{65}N_5OSi_6U$: C, 34.06; H, 7.74; N, 8.27%. Found: C, 33.58; H, 7.51; N 8.21%. ^{1}H NMR (C_6D_6, 298 K): δ –2.01 (br, s, 54H, Si(CH$_3$)$_3$), –2.97 (br, s, 2H, (H)C=C(H)), –4.89 (s, 6H, N(CH$_3$)), 25.26 (s, 3H, C(CH$_3$)) ppm. ^{29}Si {^{1}H} NMR (C_6D_6, 298 K): δ –37.74 ppm. ATR-IR ν/cm^{-1}: 2941 (s), 2892 (w), 1592 (w), 1553 (m), 1508 (w), 1416 (w), 1235 (s), 1128 (w), 984 (s), 862 (w), 823 (s), 764 (w), 747 (s), 682 (w), 660 (s), 597 (s), 478 (w), 441 (w). Note, complex **4** slowly decomposes in solution at room temperature affording [HN(SiMe$_3$)$_2$] and several unidentified products after 24 hours, as indicated by ^{1}H NMR spectroscopy.

Preparation of [U^{IV}(NSiMe$_3$)(N")$_3$][(Me)C(NMeCH)$_2$] (5)

To a cold (–78 °C) stirring dark purple solution of [U^{III}(N″)$_3$] (0.81 g, 1.00 mmol) in hexane (10 ml) was added Me_3SiN_3 (0.115 g, 1.00 mmol). The mixture was allowed to warm to room temperature slowly over 10 minutes, resulting in a colour change to dark red. The reaction mixture was stirred for 20 minutes at room temperature. After which, the volume was reduced *in vacuo* by half, and a solution of H_2C=C(NMeCH)$_2$ (0.06 g, 0.55 mmol) in toluene (5 ml) was added dropwise. The reaction mixture was stirred for 2 hours at room temperature. After which, the reaction mixture was concentrated to approximately 5 ml and stored at −30 °C for 24 hours, to afford **5** as brown needle crystals. Yield: 0.12 g, 13%. Anal. Calcd for $C_{27}H_{74}N_6Si_7U$: C, 35.34; H, 8.13; N, 9.16%. Found: C, 34.78; H, 7.91; N, 8.73%. ^{1}H NMR (C_6D_6, 298 K): δ 43.30 (s, 3H, C(CH$_3$)), –2.46 (br, s, 54H,

$Si(CH_3)_3$), –6.90 (s, 6H, $N(CH_3)$), –10.87 (s, 2H, (H)C=C(H)), –12.55 (s, 9H, (=$N(Si(CH_3)_3)$ ppm. ^{29}Si {^1H} NMR (C_6D_6, 298 K): δ –90.74 (=$N(Si(CH_3)_3)$), –131.19 (-$N(Si(CH_3)_3)$) ppm. ATR-IR ν/cm^{-1}: 2958 (m), 2918 (w), 2896 (w), 2849 (w), 1534 (m), 1409 (m), 1246 (s), 1092 (m), 1019 (s), 942 (s), 928 (w), 901 (w), 796 (s, br), 757 (s, br), 725 (w), 661 (s), 605 (s), 595 (w), 437 (w). Note, complex **5** decomposes in solution at room temperature affording [$HN(SiMe_3)_2$] and several unidentified products after 30 minutes, as indicated by ^1H NMR spectroscopy.

Electronic structure calculations

State-averaged complete active space self-consistent field spin-orbit (CASSCF-SO) calculations are performed with OpenMolcas.[62] Scalar relativistic effects are included *via* a second-order Douglas-Kroll-Hess (DKH2) Hamiltonian, which is evaluated in a basis of relativistic semi-core correlated atomic natural orbital (ANO-RCC) functions.[63,64] We use basis sets of VQZP quality on U and the first coordination sphere, and VDZP quality for all other atoms. Two electron integrals are decomposed with the Cholesky method using a threshold of 10^{-8}. CASSCF calculations are performed using a minimal active space of 2 electrons in 7 5f orbitals, averaging over 11 roots for S = 1 and 9 roots for S = 0, corresponding to the ^3H and ^1G terms, respectively. The number of optimised roots is a decisive factor, as calculations using more states fail to approach the correct high T limit of χT for both **4** and **5**; this is a result of using state-averaged molecular orbitals, where the representation of the lowest-energy states becomes less optimal as the number of averaged states increases.

ACKNOWLEDGMENTS

We gratefully acknowledge the UK EPSRC (EP/P001386/1, EP/M027015/1, EP/K024000/1), EPSRC EPR National Research Facility (NS/A000055/1) for access to SQUID magnetometry, ERC (CoG612724 and StG851504), Royal Society (UF11005 and URF191320), UK Defence Science

and Technology Laboratory (studentship to L.B.), National Nuclear Laboratory, and the University of Manchester for access to the Computational Shared Facility.

AUTHOR CONTRIBUTIONS

J.A.S. prepared and characterised the compounds. L.B. carried out and interpreted the CASSCF-SO calculations. J.A.S., E.L., and F.T. carried out and interpreted the SQUID magnetometry. A.J.W. collected, solved, and refined all the crystallographic data. N.F.C. and S.T.L. assisted with data analysis, directed the research, and wrote the manuscript with input from all the authors.

DECLARATION OF INTERESTS

The authors declare no competing interests or conflicts.

REFERENCES

1. Liddle, S. T. (2015). The renaissance of non-aqueous uranium chemistry. Angew. Chem. Int. Ed. *54*, 8604-8641.
2. Kaltsoyannis, N., and Liddle, S. T. (2016). Catalyst: nuclear power in the 21st century. Chem. *1*, 659-662.
3. Taylor, R. (2016). Reaction: a role for actinide chemists. Chem. *1*, 662-663.
4. Ion, S. (2016). Reaction: recycling and generation IV systems. Chem *1*, 663-665.
5. Day, J. P., and Venanzi, L. M. (1966). Some octahedral complexes of uranium(IV). J. Chem. Soc., A 197-200.
6. Castro-Rodríguez, I., and Meyer, K. (2006). Small molecule activation at uranium coordination complexes: control of reactivity *via* molecular architecture. Chem. Commun. 1353-1368.
7. Gardner, B. M., King, D. M., Tuna, F., Wooles, A. J., Chilton, N. F., and Liddle, S. T. (2017). Assessing crystal field and magnetic interactions in diuranium-μ-chalcogenide triamidoamine

complexes with U^{IV}-E-U^{IV} cores (E = S, Se, Te): implications for determining the presence or absence of actinide-actinide magnetic exchange. Chem. Sci. *8*, 6207-6217.

8. Rosenzweig, M. W., Heinemann, F. W., Maron, L., and Meyer, K. (2017). Molecular and electronic structure of eight-coordinate uranium bipyridine complexes: A rare example of a $Bipy^{2-}$ ligand coordinated to a U^{4+} ion. Inorg. Chem. *56*, 2792-2800.

9. Gendron, F., Le Guennic, B., and Autschbach, J. (2014). Magnetic properties and electronic structures of Ar_3U^{IV}-L complexes with Ar = $C_5(CH_3)_4H^-$ or $C_5H_5^-$ and L = CH_3, NO, and Cl. Inorg. Chem. *53*, 13174-13187.

10. Siladke, N. A., Meihaus, K. R., Ziller, J. W., Fang, M., Furche, F., Long J. R., and Evans, W. J. (2012). Synthesis, structure, and magnetism of an f element nitrosyl complex, $(C_5Me_4H)_3UNO$. J. Am. Chem. Soc. *134*, 1243-1249.

11. Hutchison, C. A., and Candela, G. A. (1957). Magnetic susceptibilities of uranium(IV) ions in cubic crystalline fields. J. Chem. Phys. *27*, 707-710.

12. Pedersen, K. S., Meihaus, K. R., Rogalev, A., Wilhelm, F., Aravena, D., Amoza, M., Ruiz, E., Long, J. R., Bendix J., and Clérac, R. (2019). $[UF_6]^{2-}$: A molecular hexafluorido actinide(IV) complex with compensating spin and orbital magnetic moments. Angew. Chem. Int. Ed. *58*, 15650-15654.

13. Gorller-Walrand C., and Binnemans, K. (1996) Handbook on the Physics and Chemistry of Rare Earths, Elsevier, vol. 23.

14. Su, J., Dau, P. D., Liu, H.-T., Huang, D.-L., Wei, F., Schwarz, W. H. E., Li, J., and Wang, L.-S. (2015). Photoelectron spectroscopy and theoretical studies of gaseous uranium hexachlorides in different oxidation states: UCl_6^{q-} (q = 0-2). J. Chem. Phys. *142*, 134308.

15. Sakurai, J. J., and Tuan, S. F. (1994). Modern quantum mechanics, Addison-Wesley Pub. Co, Reading, Mass, Rev. ed.

16. Streitwieser, A., and Müller-Westerhoff, U. (1968). Bis(cyclooctatetraenyl)uranium (uranocene). A new class of sandwich complexes that utilize atomic f orbitals. J. Am. Chem. Soc. *90*, 7364-7364.

17. Edelstein, N., Lamar, G. N., Mares F., and Streitwieser, A. (1971). Proton magnetic resonance shifts in (bis(cyclooctatetraenyl))uranium(IV). Chem. Phys. Lett. *8*, 399-402.

18. Karraker, D. G., Stone, J. A., Jones E. R., and Edelstein, N. (1970). Bis(cyclooctatetraenyl)neptunium(IV) and bis(cyclooctatetraenyl)plutonium(IV). J. Am. Chem. Soc. *92*, 4841-4845.

19. Chang, A. H. H., and Pitzer, R. M. (1989). Electronic structure and spectra of uranocene. J. Am. Chem. Soc. *111*, 2500-2507.

20. Hayes, R. G., and Edelstein, N. (1972). Elementary molecular orbital calculation on $U(C_8H_8)_2$ and its application to the electronic structures of $U(C_8H_8)_2$, $Np(C_8H_8)_2$, and $Pu(C_8H_8)_2$. J. Am. Chem. Soc. *94*, 8688-8691.

21. Warren, K. D. (1975). Ligand field theory of metal sandwich complexes. Magnetic properties of f^x configurations. Inorg. Chem. *14*, 3095-3103.

22. Newell, B. S., Rappé, A. K., and Shores, M. P. (2010). Experimental evidence for magnetic exchange in di- and trinuclear uranium(IV) ethynylbenzene complexes. Inorg. Chem. *49*, 1595-1606.

23. Fortier, S., Melot, B. C., Wu, G., and Hayton, T. W. (2009). Homoleptic uranium(IV) alkyl complexes: synthesis and characterization. J. Am. Chem. Soc. *131*, 15512-15521.

24. Chadwick, F. M., Ashley, A., Wildgoose, G., Goicoechea, J. M., Randall, S., and O'Hare, D. (2010). Bis(permethylpentalene)uranium. Dalton Trans. *39*, 6789-6793.

25. Seaman, L. A., Fortier, S., Wu, G., and Hayton T. W. (2011). Comparison of the redox chemistry of primary and secondary amides of U(IV): isolation of a U(VI) bis(imido) complex or a homoleptic U(VI) amido complex. Inorg. Chem. *50*, 636-646.

26. Fortier, S., Brown, J. L., Kaltsoyannis, N., Wu, G., and Hayton, T. W. (2012). Synthesis, molecular and electronic structure of $U^{V}(O)[N(SiMe_3)_2]_3$. Inorg. Chem. *51*, 1625-1633.

27. Brown, J. L., Fortier, S., Lewis, R. A., Wu, G., and Hayton, T. W. (2012). A complete family of terminal uranium chalcogenides, $[U(E)(N\{SiMe_3\}_2)_3]^-$ (E = O, S, Se, Te). J. Am. Chem. Soc. *134*, 15468-15475.

28. Patel, D., Tuna, F., McInnes, E. J. L., Lewis, W., Blake, A. J., and Liddle, S. T. (2013). An Actinide-Zintl Cluster: A tris(triamidouranium)μ_3-η^2:η^2:η^2-heptaphosphanortricyclane and its diverse synthetic utility. Angew. Chem. Int. Ed. *52*, 13334-13337.

29. Lewis, A. J., Williams, U. J., Carroll, P. J., and Schelter, E. J. (2013). Tetrakis(bis(trimethylsilyl)amido)uranium(IV): synthesis and reactivity. Inorg. Chem. *52*, 7326-7328.

30. Gardner, B. M., Balázs, G., Scheer, M., Tuna, F., McInnes, E. J. L., McMaster, J., Lewis, W., Blake, A. J., and Liddle, S. T. (2014). Triamidoamine-uranium(IV)-stabilized terminal parent phosphide and phosphinidene complexes. *Angew. Chem. Int. Ed. 53*, 4484-4488.

31. King, D. M., McMaster, J., Tuna, F., McInnes, E. J. L., Lewis, W., Blake, A. J., and Liddle, S. T. (2014). Synthesis and characterization of an f-block terminal parent imido [U=NH] complex: a masked uranium(IV)-nitride. J. Am. Chem. Soc. *136*, 5619-5622.

32. Halter, D. P., La Pierre, H. S., Heinemann, F. W., and Meyer, K. (2014). Uranium(IV) halide (F^-, Cl^-, Br^-, I^-) monoarene complexes. Inorg. Chem. *53*, 8418-8424.

33. Gardner, B. M., Balázs, G., Scheer, M., Tuna, F., McInnes, E. J. L., McMaster, J., Lewis, W., Blake, A. J., and Liddle, S. T. (2015). Triamidoamine uranium(IV)-arsenic complexes containing one-, two-, and three-fold U-As bonding interactions. Nat. Chem. *7*, 582-590.

34. Rookes, T. M., Gardner, B. M., Balázs, G., Gregson, M., Tuna, F., Wooles, A. J., Scheer, M., and Liddle, S. T. (2017). Crystalline diuranium-phosphinidiide and -μ-phosphido complexes with symmetric and asymmetric UPU cores. Angew. Chem. Int. Ed. *56*, 10495-10500.

35. Gregson, M., Lu, E., Mills, D. P., Tuna, F., McInnes, E. J. L., Hennig, C., Scheinost, A. C., McMaster, J., Lewis, W., Blake, A. J., Kerridge, A., and Liddle, S. T. (2017). The inverse-*trans*-influence in tetravalent lanthanide and actinide *bis*(carbene) complexes. Nat. Commun. *8*, 14137.

36. Lu, E., Boronski, J. T., Gregson, M., Wooles, A. J., and Liddle, S. T. (2018). Silyl-phosphino-carbene complexes of uranium(IV). Angew. Chem. Int. Ed. *57*, 5506-5511.

37. Lu, E., Wooles, A. J., Gregson, M., Cobb, P. J., and Liddle, S. T. (2018). A very short uranium(IV)-rhodium(I) bond with net double-dative bonding character. Angew. Chem. Int. Ed. *57*, 6587-6591.

38. Boronski, J. T., Doyle, L. R., Seed, J. A., Wooles, A. J., and Liddle, S. T. (2020). f-Element half-sandwich complexes: a tetrasilylcyclobutadienyl-uranium(IV)-tris(tetrahydroborate) anion pianostool complex. Angew. Chem. Int. Ed. *59*, 295-299.

39. Seed, J. A., Sharpe, H. R., Futcher, H. J., Wooles, A. J., and Liddle, S. T. (2020). Nature of the arsonium-ylide $Ph_3As{=}CH_2$ and a uranium(IV) arsonium-carbene complex. Angew. Chem. Int. Ed. *59*, 15870-15874.

40. Seed, J. A., Gregson, M., Tuna, F., Chilton, N. F., Wooles, A. J., McInnes, E. J. L., and Liddle, S. T. (2017). Rare-earth- and uranium-mesoionic carbenes: a new class of f-block carbene complex derived from an N-heterocyclic olefin. Angew. Chem. Int. Ed. *56*, 11534-11538.

41. Fortier, S., Kaltsoyannis, N., Wu, G., and Hayton, T. W. (2011). Probing the reactivity and electronic structure of a uranium(V) terminal oxo complex. J. Am. Chem. Soc. *133*, 14224-14227.

42. Windorff, C. J., and Evans, W. J. (2014). ^{29}Si NMR spectra of silicon-containing uranium complexes. Organometallics *33*, 3786-3791.

43. Mills, D. P., Moro, F., McMaster, J., Van Slageren, J., Lewis, W., Blake, A. J., and Liddle, S. T. (2011). A delocalized arene-bridged diuranium single-molecule magnet. Nat. Chem. *3*, 454-460.

44. Zalkin, A., Brennan, J. G., and Andersen, R. A. (1988). Tris[bis(trimethylsilyl)amido](trimethylsilylimido)uranium(V). Acta Cryst. Sect. C *44*, 1553-1554.

45. Smiles, D. W., Wu, G., and Hayton, T. W. (2013). Synthesis of uranium-ligand multiple bonds by cleavage of a trityl protecting group. J. Am. Chem. Soc. *136*, 96-99.

46. Jilek, R. E., Tomson, N. C., Shook, R. L., Scott, B. L., and Boncella, J. M. (2014). Preparation and reactivity of the versatile uranium(IV) imido complexes $U(NAr)Cl_2(R_2bpy)$ (R = Me, ^{t}Bu) and $U(NAr)Cl_2(tppo)_3$. Inorg. Chem. *53*, 9818-9826.

47. Mullane, K. C., Lewis, A. J., Yin, H., Carroll, P. J., and Schelter, E. J. (2014). Anomalous one-electron processes in the chemistry of uranium nitrogen multiple bonds. Inorg. Chem. *53*, 9129-9139.

48. Kindra, D. R., and Evans, W. J. (2014). Magnetic susceptibility of uranium complexes. Chem. Rev. *114*, 8865-8882.

49. Todorova, T. K., Gagliardi, L., Walensky, J. R., Miller K. A., and Evans, W. J. (2010). DFT and CASPT2 analysis of polymetallic uranium nitride and oxide complexes: How theory can help when X-ray analysis is inadequate. J. Am. Chem. Soc. *132*, 12397-12403.

50. Spivak, M., Vogiatzis, K. D., Cramer, C. J., De Graaf C., and Gagliardi, L. (2017). Quantum chemical characterization of single molecule magnets based on uranium. J. Phys. Chem. A *121*, 1726-1733.

51. King, D. M., Cleaves, P. A., Wooles, A. J., Gardner, B. M., Chilton, N. F., Tuna, F., Lewis, W., McInnes E. J. L., and Liddle, S. T. (2016). Molecular and electronic structure of terminal and alkali metal-capped uranium(V)-nitride complexes. Nat. Commun. *7*, 13773.

52. Stevens, K. W. H. (1952). Matrix elements and operator equivalents connected with the magnetic properties of rare earth ions. Proc. Phys. Soc. Sect. A *65*, 209-215.

53. Abragam, A., and Bleaney, B. (1970). Electron Paramagnetic Resonance of Transition Ions, Oxford University Press.

54. Ungur, L., and Chibotaru, L. F. (2017). Ab initio crystal field for lanthanides. Chem. Eur. J. *23*, 3708-3718.

55. Chilton, N. F., Anderson, R. P., Turner, L. D., Soncini A., and Murray, K. S. (2013). PHI: a powerful new program for the analysis of anisotropic monomeric and exchange-coupled polynuclear d- and f-block complexes. J. Comp. Chem. *34*, 1164-1175.

56. Chibotaru, L. F. and Ungur, L. (2012). Ab initio calculation of anisotropic magnetic properties of complexes. I. unique definition of pseudospin hamiltonians and their derivation. J. Chem. Phys. *137*, 064112.

57. King, D. M., Tuna, F., McMaster, J., Lewis, W., Blake, A. J., McInnes E. J. L., and Liddle, S. T. (2013). Single-molecule magnetism in a single-ion triamidoamine uranium(V) terminal mono-oxo complex. Angew. Chem. Int. Ed. *52*, 4921-4924.

58. Rinehart, J. D., and Long, J. R. (2011). Exploiting single-ion anisotropy in the design of f-element single-molecule magnets. Chem. Sci. *2*, 2078-2085.

59. Chilton, N. F., Collison, D., McInnes, E. J. L., Winpenny R. E. P., and Soncini, A. (2013). An electrostatic model for the determination of magnetic anisotropy in dysprosium complexes. Nat. Commun. *4*, 2551.

60. Chilton, N. F. (2015). Design criteria for high-temperature single-molecule magnets. Inorg. Chem. *54*, 2097-2099.

61. Sievers, J. (1982). Asphericity of 4f-shells in their Hund's rule ground states. Zeitschrift für Physik B Condensed Matter *45*, 289-296.

62. Fernández Galván, I., Vacher, M., Alavi, A., Angeli, C., Aquilante, F., Autschbach, J., Bao, J. J., Bokarev, S. I., Bogdanov, N. A., Carlson, R. K., Chibotaru, L. F., Creutzberg, J., Dattani,

N., Delcey, M. G., Dong, S. S., Dreuw, A., Freitag, L., Frutos, L. M., Gagliardi, L., Gendron, F., Giussani, A., Gonzalez, L., Grell, G., Guo, M., Hoyer, C. E., Johansson, M., Keller, S., Knecht, S., Kovačević, G., Källman, E., Li Manni, G., Lundberg, M., Ma, Y., Mai, S., Malhado, J. P., Malmqvist, P. A., Marquetand, P., Mewes, S. A., Norell, J., Olivucci, M., Oppel, M., Phung, Q. M., Pierloot, K., Plasser, F., Reiher, M., Sand, A. M., Schapiro, I., Sharma, P., Stein, C. J., Sørensen, L. K., Truhlar, D. G., Ugandi, M., Ungur, L., Valentini, A., Vancoillie, S., Veryazov, V., Weser, O., Wesolowski, T. A., Widmark, P.-O., Wouters, S., Zech, A., Zobel J. P., and Lindh, R. (2019). OpenMolcas: From source code to insight. J. Chem. Theory Comp. *15*, 5925-5964.

63. Roos, B. O., Lindh, R., Malmqvist, P.-Å., Veryazov V., and Widmark, P.-O. (2004). Main group atoms and dimers studied with a new relativistic ANO basis set. J. Phys. Chem. A *108*, 2851-2858.

64. Roos, B. O., Lindh, R., Malmqvist, P.-Å., Veryazov V., and Widmark, P.-O. (2005). New relativistic ANO basis set for actinide atoms. Chem. Phys. Lett. *409*, 295-299.

FIGURE AND SCHEME TITLES AND LEGENDS

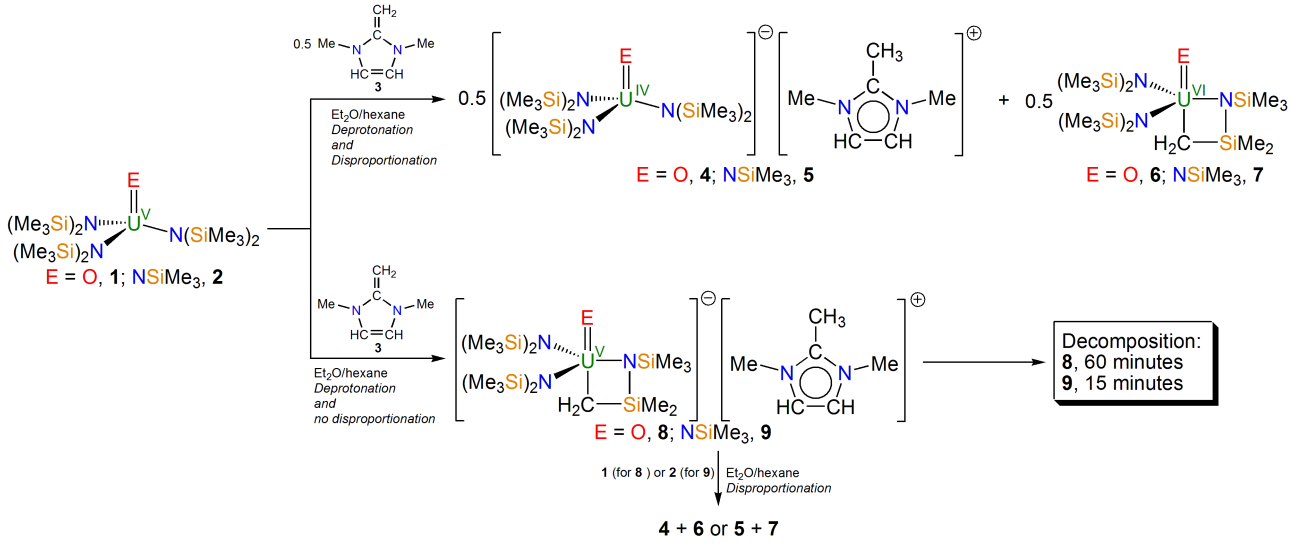

Scheme 1. Synthesis of 4 and 6 or 5 and 7 from 1 or 2, respectively, when treated with half an equivalent of 3. Conversely, treatment of **1** or **2** with one equivalent of **3** results in formation of **8**

or **9**, respectively. Mixtures of **8** and **9** decompose rapidly, with the times quoted being for total decomposition, but if one further equivalent of **1** or **2**, for **8** or **9** respectively, is already present or added rapidly then 1:1 mixtures of **4** and **6** or **5** and **7** are obtained.

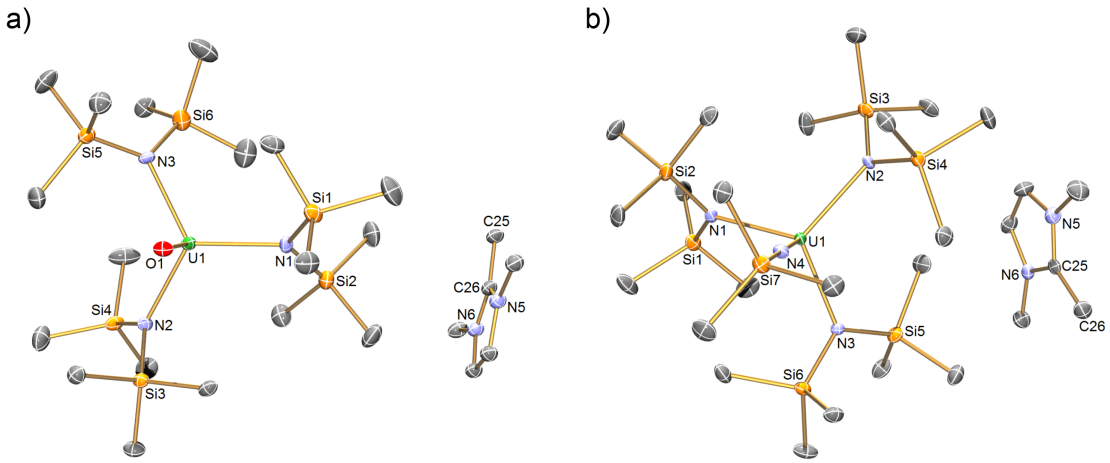

Figure 1. Solid state structures of a) 4 and b) 5 at 150 K with selective labelling. Displacement ellipsoids set at 30% with hydrogen atoms and minor disordered components omitted for clarity.

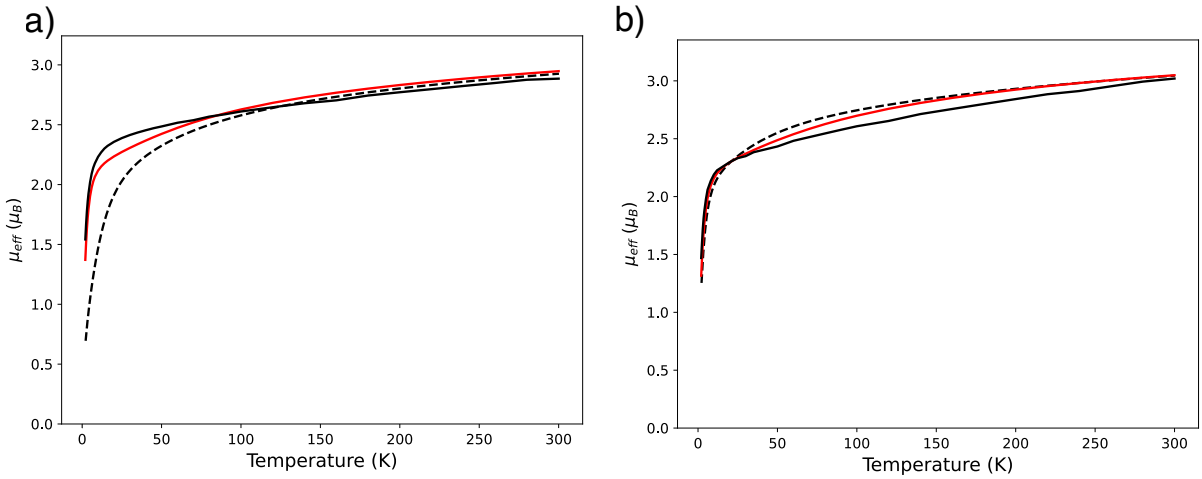

Figure 2. Magnetic moment as a function of temperature for a) 4 and b) 5, recorded in a field of 0.5 T (black solid lines). Dotted black lines are calculated by CASSCF(2,7)-SO (11 triplets + 9 singlets, see Experimental Procedures and Supplemental Information for details) and solid red lines are the best fits with a CF Hamiltonian (using CASSCF(2,7)-SO-calculated parameters) with optimisation of a single parameter (a: B_6^6, b: B_6^3).

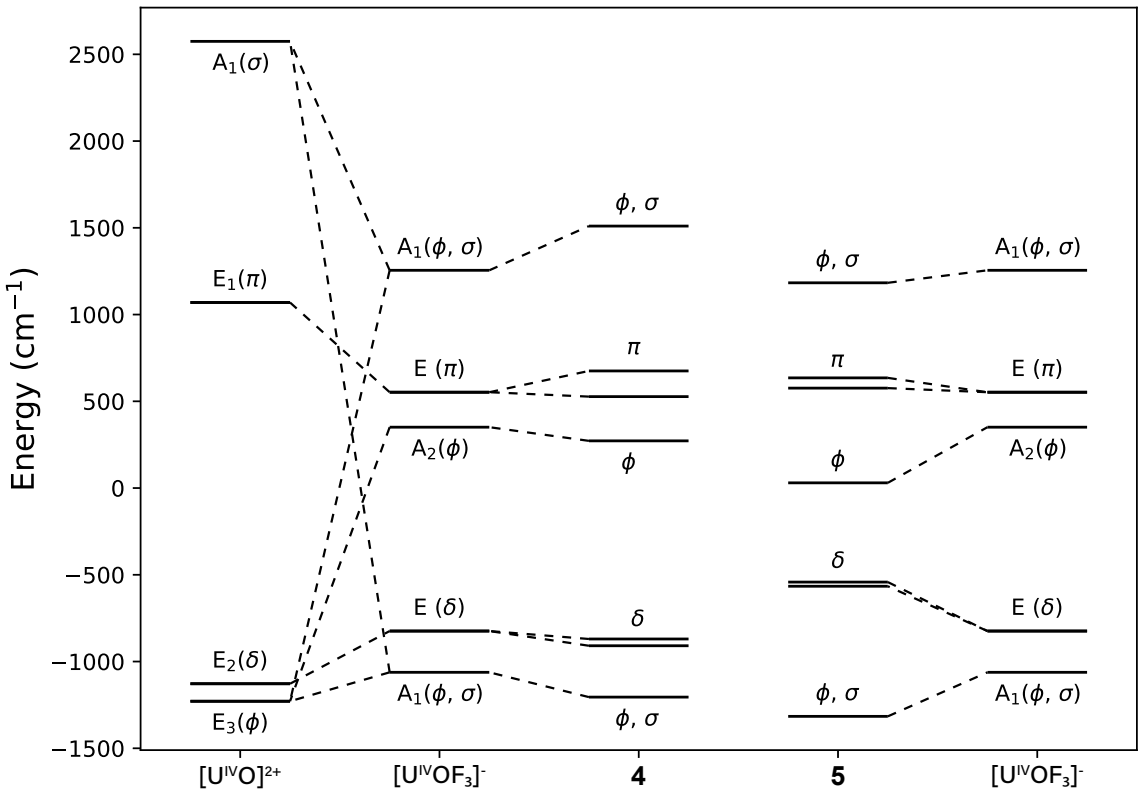

Figure 3. Energies of the 5f orbitals derived using the Stevens operator equivalent method. This is based on the effective crystal field splitting of the $^3H_4$ ground term calculated with CASSCF(2,7)-SO (11 triplets + 9 singlets, see Experimental Procedures and Supplemental Information for details). Only dominant contributions to the orbitals of $[U^{IV}OF_3]^-$, **4** and **5** are given.

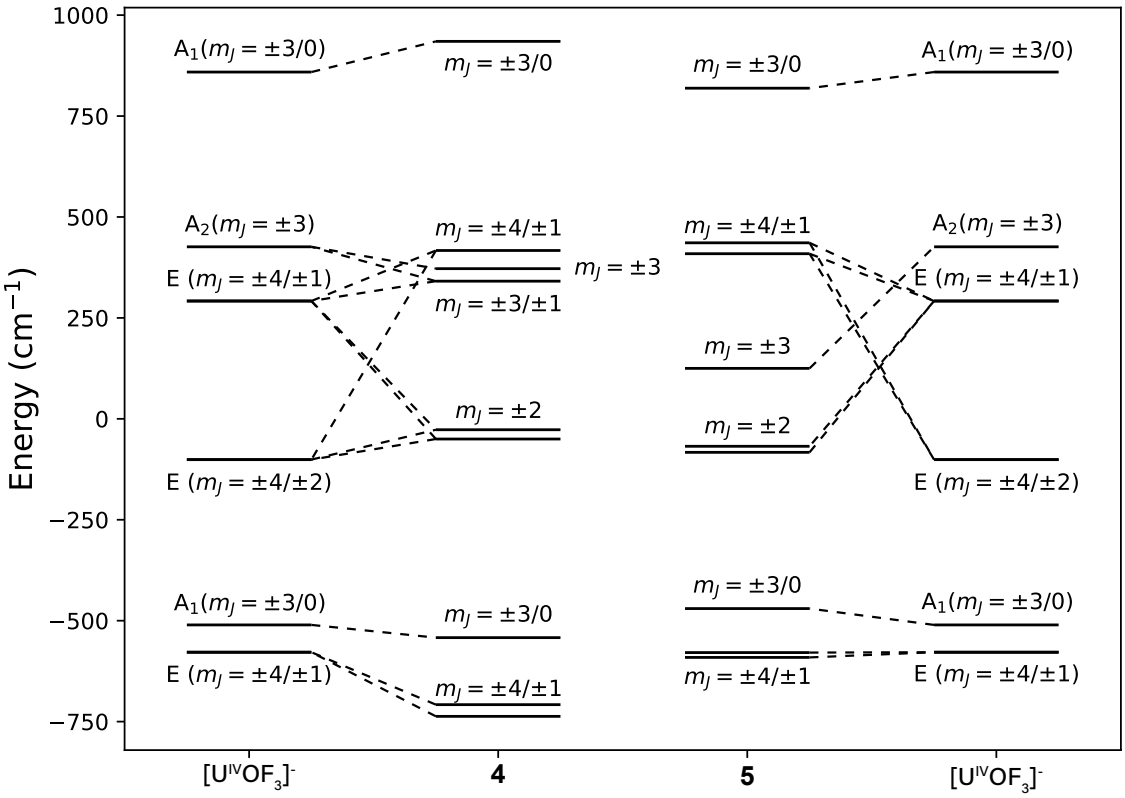

Figure 4. Energies of CF states arising from the $^3H_4$ ground term. Calculated with CASSCF(2,7)-SO (11 triplets + 9 singlets, see Experimental Procedures and Supplemental Information for details). Only dominant contributions to the states are shown.

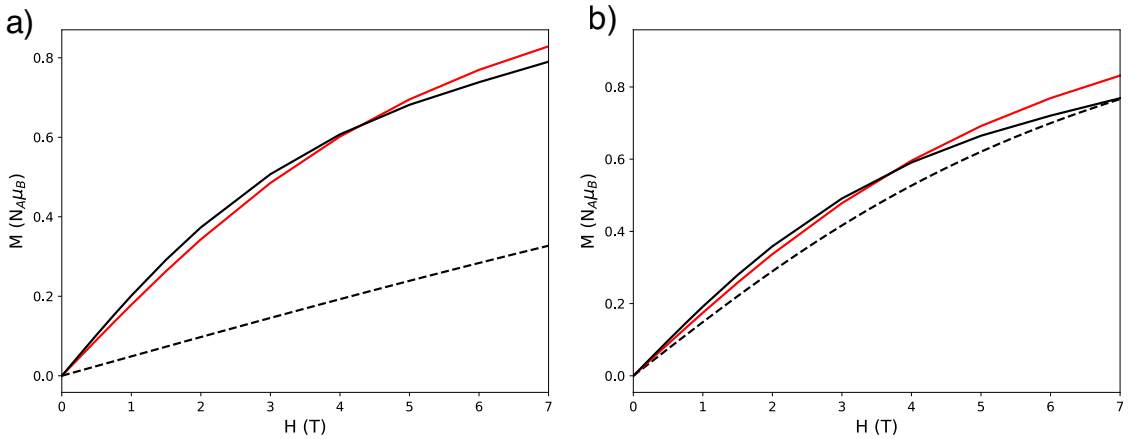

Figure 5. Magnetisation at 4 K as a function of field for a) 4 and b) 5 (black solid lines). Dotted black lines are calculated by CASSCF(2,7)-SO (11 triplets + 9 singlets, see Experimental Procedures and Supplemental Information for details) and solid red lines are the best fits with a CF

Hamiltonian (using CASSCF(2,7)-SO-calculated parameters) with optimisation of a single parameter (a: B_6^6, b: B_6^3).

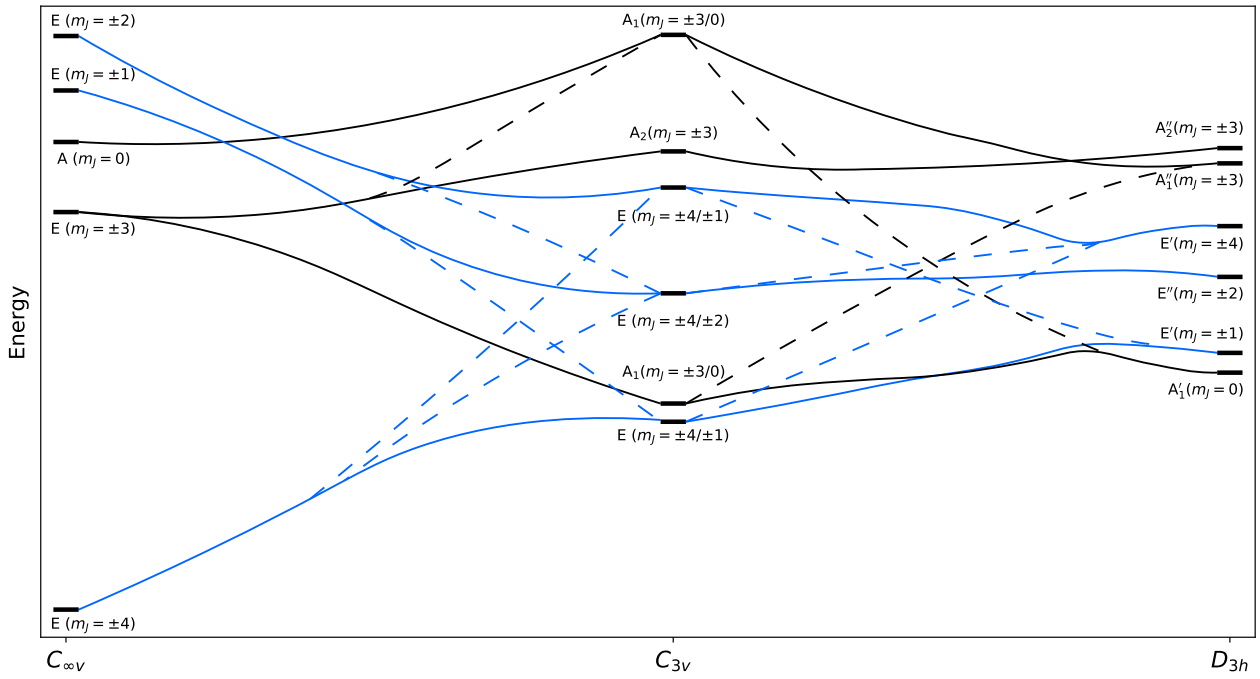

Figure 6. Energies of CF states for a model complex of $[U^{IV}OF_3]^-$. The U-F bond lengths are reduced from 47 Å ($C_{\infty v}$, left) to 2.348 Å (C_{3v}, centre), and the U-O bond length is increased from 1.884 Å (C_{3v}, centre) to 38 Å (D_{3h}, right). Doubly-degenerate E states are coloured blue and singly-degenerate A states are coloured black. Only dominant contributions to the states are shown.

ToC Entry